

Effat University Repository

The Life Distribution of Commercial Concentrator III-V Triple-Junction Solar Cells in View of Inverse Power law and Arrhenius Life

Item Type	Thesis
Authors	Dennah, Dunya
Publisher	Effat University
Download date	2026-05-16 09:02:45
Link to Item	http://hdl.handle.net/20.500.14131/92

EFFAT UNIVERSITY
COLLEGE OF ENGINEERING
DEPARTMENT OF ELECTRICAL AND COMPUTER ENGINEERING



جامعة عفت
EFFAT UNIVERSITY

The Life Distribution of Commercial Concentrator III–V Triple-Junction Solar Cells in View of Inverse Power law and Arrhenius Life-Stress Relationships in Terrestrial and Space

A Thesis Submitted For the Requirements of the Degree of Master of Science in Energy Engineering

By:

Dunya Dannah
dydanah@effat.edu.sa

Supervised by

Dr. Omar Kitaneh
Associate Professor, Director of Natural Science, Math and Technology Unit Effat College of Engineering
okitaneh@effatuniversity.edu.sa

Dr. Mohammed Abdulmajid
Assistant Professor and Researcher Effat College of Engineering Electrical and Computer Engineering Department
moabdulmajid@effatuniversity.edu.sa

Jeddah, Kingdom of Saudi Arabia
May 2022 – Shawal 1444

جامعة عفت
كلية الهندسة
قسم هندسة الكهرباء وهندسة الحاسبات



جامعة عفت
EFFAT UNIVERSITY

توزيع الحياة للخلايا الشمسية المركزة التجارية
ثلاثية الوصلات في ضوء قانون الطاقة المعكوس وعلاقات أرهينوس بين الحياة والإجهاد في الأرض
والفضاء

أطروحة مقدمة لمتطلبات درجة ماجستير العلوم في هندسة الطاقة

دنيا يحيي دنه

إشراف

د. عمر كتانة

أستاذ مشارك

وحده العلوم الطبيعية والرياضيات والتقنية

كلية الهندسة – جامعة عفت

okitanneh@effatuniversity.edu.sa

د. محمد عبدالمجيد

أستاذ مساعد و باحث علمي

قسم الهندسة الكهربائية وهندسة الحاسبات

كلية الهندسة – جامعة عفت

moabdulmajid@effatuniversity.edu.sa

جدة، المملكة العربية السعودية
شوال 1443 هـ – مايو 2022 م

Signature Page

**Effat University
Jeddah, Saudi Arabia**

Deanship of Graduate Studies and Research

This thesis, written by Dunya Dannah under the direction of his/her thesis supervisor and approved by his/her thesis committee, has been presented to and accepted by the Dean of Graduate Studies and Research on Renewable Energy Engineering in partial fulfillment of the requirements for the degree of MASTER OF SCIENCE in 10th April,2022

Thesis Committee

Thesis Supervisor

Name:

Signature:

Co-supervisor/member

Name:

Signature:

External Member

Name:

Signature:

Member

Name:

Signature:

Department Chair

Name:

Signature:

Dean of the College

Name:

Signature:

Dean of Graduate Studies & Research

Name:

Signature:

Arabic Signature Page

جامعة عفت
جدة، المملكة العربية السعودية
عمادة الدراسات العليا والبحث العلمي

قام بكتابة هذه الرسالة الطالب / الطالبة دنيا يحيى دنه ، تحت إشراف المشرف المكلف بالإشراف على رسالته / رسالتها، وتم إجازتها من قبل لجنة التحكيم، وتم تقديمها إلى عمادة الدراسات العليا والبحث العلمي بجامعة عفت، كجزء من متطلبات الحصول على درجة الماجستير في العلوم، برنامج هندسة الطاقة المتجددة وقد تم الموافقة على الرسالة وإجازتها بتاريخ:

أعضاء لجنة التحكيم

المشرف على الرسالة
الاسم :
التوقيع:

المشرف المشارك
الاسم :
التوقيع:

العضو الخارجي
الاسم :
التوقيع:

العضو
الاسم :
التوقيع:

رئيس القسم
الاسم :
التوقيع:

عميدة الكلية
الاسم :
التوقيع:

عميدة الدراسات العليا والبحث العلمي
الاسم :
التوقيع:

DECLARATION

I hereby declare that this thesis titled "*The Life Distribution of Commercial Concentrator III–V Triple-Junction Solar Cells in View of Inverse Power law and Arrhenius Life-Stress Relationships in Terrestrial and Space* " is based on my original work except for quotations and citations been duly acknowledged. I also declare that the proposed dissertation has not been previously or concurrently submitted for the award of any degree at Effat University, or any other university or institution. I grant the copyrights of this Dissertation/Thesis to Effat University to be copied in whole or in part without further reference to me. This permission covers only single copies made for study purposes, subject to acknowledgment. I also permit electronic upload to BlackBoard of a copy of my Dissertation/Thesis.

Student Name: Dunya Yahya Dannah

Signature: DUNYA DENNAH

Date: 17th May,2022

ACKNOWLEDGEMENTS

I would like to thank the following people, without whom I would not have been able to complete this research and without whom I would not have made it through my master's degree!

The Energy Engineering department team at EFFAT University, especially my supervisors, **Dr. Mohammed Abdulmajid** and **Dr. Omar Kitanneh**, whose insight and knowledge into the subject matter steered me through this research, and special thanks to **Salwa Ammach**, who supported this research.

And my biggest thanks to my Mother, **Laila Fakiha**, for all the support you have shown me through this research, the culmination of two years of distance learning. For my daughter, **Sulafa Ganadeli**, sorry for being even grumpier than normal whilst I wrote this thesis! Thanks for all your support, without which I would have stopped these studies a long time ago; you have been amazing.

The Life Distribution of Commercial Concentrator III–V Triple-Junction Solar Cells in View of Inverse Power law and Arrhenius Life-Stress Relationships in Terrestrial and Space

Abstract

Renewable energy is one of the essential clean power sources, especially solar energy. The world is shifting toward increasing production from clean energy with a vast transformation level of integrating solar energy with grid production. This comprehensive transformation leads the researchers to focus more on solar reliability, which is considered one of the most challenging elements of solar power to increase production with the highest quality. Different factors affect the PV panel's estimated lifetime before the failure accrues, such as temperature stress, voltage, irradiation, and many other factors.

PV panel output power will be a certain percentage of its original Standard Test Condition (STC), rated DC power, depending on its working hours, or we can say PV panel age. The consumer must trust and be confident in such PV manufacturers' companies to ensure the system will remain stable and reliable for a long time before the decision is taken, which is what they call a warranty. PV panels are still being replaced and repaired before the expiration of their warranty period.

Studying the PV model's reliability will limit the PV panel's failure and ensure a long lifetime for the system to operate and produce efficient and reliable power. The accelerated lifetime ALT for the PV will simulate the failure under different stressor conditions with the minimum period.

This research will use the Inverse power Law module based on statistical analysis with different distributions such as Weibull and Lognormal. Previous studies were done in the same field using the Arrhenius model. Authors usually used Arrhenius as the best life-stress relationship; others favored the inverse power law in many accelerated life-testing experiments even when the stress is thermal. The same procedures and analysis were done in this research by testing the result of ALT space solar cells to support this theory; more details are described in the below report sections.

Keywords: Accelerated life test; Concentration photovoltaic systems; Solar cells; Weibull distribution; Lognormal; Inverse power law life-stress relationship; Arrhenius life-stress relationship; space solar cells; Renewable energy.

توزيع الحياة للخلايا الشمسية المركزة التجارية
ثلاثية الوصلات في ضوء قانون الطاقة المعكوس وعلاقات أرهينوس بين الحياة والإجهاد في الأرض والفضاء

Arabic Abstract

الطاقة المتجددة هي أحد مصادر الطاقة النظيفة الأساسية ، وخاصة الطاقة الشمسية. يتحول العالم نحو زيادة الإنتاج من الطاقة النظيفة مع مستوى تحول واسع لدمج الطاقة الشمسية مع إنتاج الشبكة. يقود هذا التحول الشامل الباحثين إلى التركيز أكثر على موثوقية الطاقة الشمسية ، والتي تعتبر أحد أكثر عناصر الطاقة الشمسية تحدياً لزيادة الإنتاج بأعلى جودة. تؤثر العوامل المختلفة على الوقت الحي المقدر للوحة الكهروضوئية قبل تراكم الفشل ، مثل إجهاد درجة الحرارة والجهد والإشعاع والعديد من العوامل الأخرى.

ستكون طاقة خرج اللوحة الكهروضوئية عبارة عن نسبة مئوية معينة من حالة الاختبار القياسية الأصلية. تصنيف طاقة التيار المستمر ، اعتماداً على ساعات التشغيل ، بمعنى آخر ، عمر اللوحة الكهروضوئية. يجب أن يثق المستهلك ويثق في شركات مصنعي الكهروضوئية هذه لضمان بقاء النظام مستقرًا وموثوقًا به لفترة طويلة قبل اتخاذ القرار ، وهو ما يسمونه الضمان. على الرغم من استمرار استبدال الألواح الكهروضوئية وإصلاحها قبل انتهاء فترة الضمان الخاصة بها.

ستؤدي دراسة موثوقية النموذج الكهروضوئي إلى الحد من فشل اللوحة الكهروضوئية وتضمن عمراً طويلاً للنظام للعمل وإنتاج طاقة فعالة وموثوقة. سوف يحاكي العمر الافتراضي المتسارع للفشل في ظل ظروف الضغط المختلفة بأقل فترة.

استخدم المؤلفون عادة أرهينوس كأفضل علاقة لضغوط الحياة ، بينما فضل آخرون قانون القوة العكسية في العديد من تجارب اختبار الحياة المعجلة حتى عندما يكون الإجهاد حرارياً. تم إجراء نفس الإجراءات والتحليلات في هذا البحث من خلال اختبار نتيجة اختبار الحياة المعجل للخلايا الشمسية الفضائية لدعم هذه النظرية ، تم وصف المزيد من التفاصيل في أقسام التقرير أدناه

الكلمات المفتاحية: اختبار الحياة المعجل؛ أنظمة تركيز الخلايا الكهروضوئية؛ الخلايا الشمسية؛ توزيع ويبل؛ قانون السلطة العكسية علاقة ضغوط الحياة ؛ علاقة أرهينوس بضغوط الحياة؛ خلايا شمسية ضوئية؛ الطاقة المتجددة.

Table of Content

Signature page	03
Arabic Signature page	04
Declaration	05
Acknowledgment	06
Abstract	07
Arabic Abstract	08
1. Chapter 1: Introduction	10
1.1 Research Question	12
1.2 Methodology	13
1.3 Research Objective	13
2. Chapter 2: Literature Review	14
2.1 Solar Energy	14
2.2 Multi-Junction Solar Cells (MJSC)	15
2.3 Concentrated Photovoltaic	17
2.3.1 5 junction Photovoltaic	18
2.4 Space Photovoltaic.....	21
2.5 Terrestrial Accelerated Life Test (ALT).....	21
2.6 Space Accelerated Life Test (ALT)	22
2.7 Reliability and statics	22
2.8.1 Weibull Distribution	24
2.8.2 Lognormal Distribution	25
3. Chapter 3: Result / Findings	27
3.1 Terrestrial PV Results	27
3.1.1 Predicting the Life at Uses condition Using IPL and Arrhenius Models.....	27
3.2 Space PV Results	30
3.2.1 Predicting the Life at Uses condition Using IPL and Arrhenius Models.....	33
4. Chapter 4: Discussion	36
5. Chapter 5: Conclusion	37
References	38
List of Figures	41
List of Tables	42
List of Terms	43
Appendices	44

Chapter 1

1. Introduction

Renewable energy is the future worldwide source goal to get electricity. Conventional energy sources are non-environmentally friendly sources that will cause CO₂ emissions, leading to increased atmospheric temperature. Many types of renewable sources can produce clean energy, but we will focus on solar energy in this research. We've all heard about the potential of solar power. It's cleaner, more sustainable, and better for the environment than fossil fuels like coal and oil. In addition, fortunately for us, solar energy is becoming more accessible to us as prices continue to fall. It is not just cleanliness that makes solar power so great - it also seems to be an excellent option for those who live in lower-income communities or regions with less access to grid electricity.

Solar energy is a vast field to study. We have different mechanisms to get electricity from solar, either from converting photons into electricity or concentrated heating. For example, standard Photovoltaic (PV) takes energy from the sunlight that is absorbed by the PV cells in the panel. This energy creates electrical charges that respond to an internal electric field in the cell, causing electricity to flow.

In this research, we will focus on the new technology of solar energy (concentrated photovoltaic) CPV, that comping Photovoltaic technology uses sunlight to generate electricity. Unlike traditional photovoltaic systems, it focuses sunlight into small, highly efficient multi-junction solar cells (MJSC) using lenses or curved mirrors[1]. Refer to figure 1.

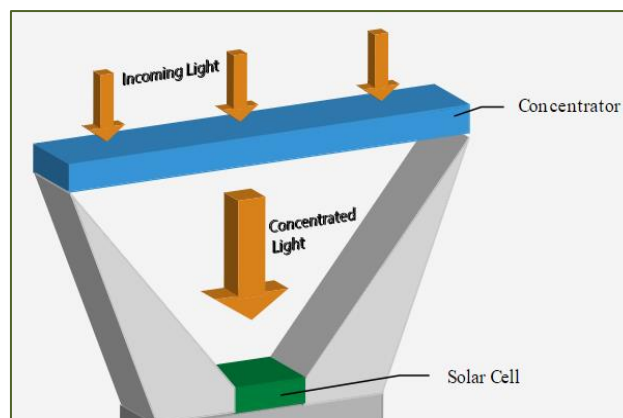


Fig.1 Concentrated Photovoltaics general diagram[2].

PV technologies can convert 15% to 18% percent of incident solar radiation into electricity, transforming the rest to heat. Many limitations and high costs to convert energy based on silicon material lead to looking into concentrated PV with multijunction material are premised on the idea of increasing the rate of incident solar radiation on a small area via employing optical components such as lenses and mirrors to maximize the energy [3]. Multi-Junction Solar cells have several p-n junctions composed of semiconductor materials. In response to different wavelengths of light, the p-n Junction of each material will produce an electric current. According to National Renewable Energy Laboratory (NREL), the highest efficiency is 46% for 3 and 4 MJSC at 25 °C, as shown in figure 2 [4].

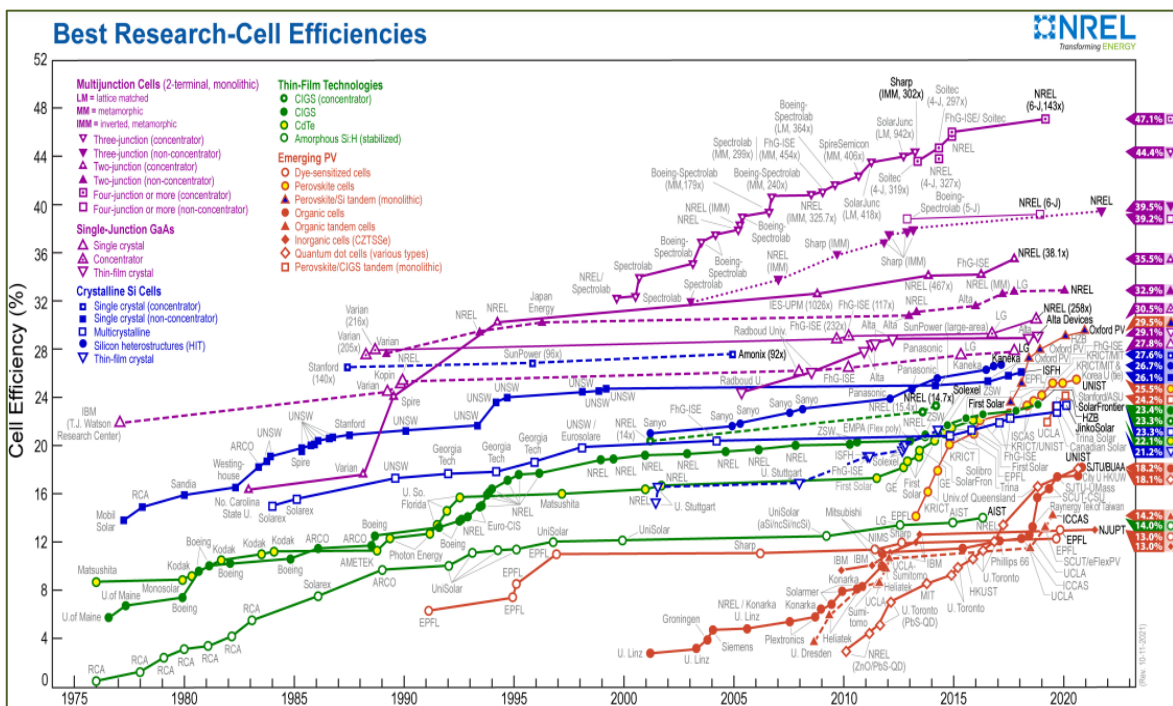


Fig.2 NREL highest confirmed conversion efficiencies for research cells for a range of photovoltaic technologies, plotted from 1976 to the present [4]

Like any other system in power generation applications, reliability is critical. Terrestrial and Space Solar panels are crucial elements exposed to the harsh environment surrounding them to supply the cells by photons to convert them into electric power. Increasing the reliability of the CPV is one of the most challenging and promising topics for the researcher. CPV needs a long time, around 25 years, to be studied to know the estimated lifetime for the system, which will require a long time to wait for the data to perform a reliability assessment.

Accelerated life test ALT is needed for this study to enable engineers to quantify the product's life features and make comprehensive predictions about the CPV to get the data in an acceptable time shorter than normal conditions[5]. This work analyzes real data produced by ALT using two statistical distributions (Weibull and Lognormal) based on inverse power law. In addition, we compare the result with the Arrhenius model, which has been studied before. As the Arrhenius model is sensitive to the activation energy, we will utilize the inverse power law as a simpler life-stress relationship and compare the predictions of the CPV lifetime obtained using both models when the CPV are used for terrestrial and in space applications.

1.1 Research Questions

This research aims to study methods to estimate the terrestrial and space triple junction concentrated solar-based accelerated lifetime test (ALT) under multiple thermal stresses by using statistical probability distributions, Weibull, and lognormal distributions in view of the Inverse power law and compare it with Arrhenius model that another previous work has addressed. In the end, we will try to answer the following two questions:

- Can we estimate the lifetime for Concentrated Photovoltaic based on inverse power law?
- Do the lifetimes of CPVs in space, and terrestrial follow the same model?

1.2 Research Methodology

- Check the goodness of fit test of some experimental data sets to fit Weibull and Lognormal distributions and maybe other distributions
- Estimate the parameters of each distribution using the proper method, possibly using maximum likelihood estimates (MLE)
- Extrapolate the lifetime under nominal conditions using the inverse power law
- Compare the lifetime distribution obtained from inverse power law with that of Arrhenius
- The data sets that will be considered are terrestrial and space CPVs
- The calculation will be implemented using MATLAB, a powerful computational program, and Mathematica, a high-performing symbolic package.

1.3 Research Objective

The main objective of this research is to compare the predictions for the lifetime of commercial concentrated photovoltaic three junction solar cells at use conditions, which are estimated using two common life-stress relationships, Arrhenius and Inverse power law. The results are built based on real data of accelerated lifetimes obtained from standard accelerated lifetime tests (ALT). The terrestrial and space environmental conditions are emulated, where the data is proved to follow flexible probabilistic models, the Weibull and Lognormal distributions.

2. Literature Review

2.1 Solar Energy

The Sun is an endless energy supply that can meet humanity's energy requirements. The Sun's energy may be transformed into electricity or immediately utilized. Sun energy may create electricity either directly through photovoltaic (PV) cells or indirectly through concentrated solar power (CSP).

Photovoltaic, a term used to describe a device that converts solar radiation into electrical energy, is integral to the power grid. It falls under the category of renewable energy, meaning it doesn't pollute or contribute to greenhouse gas emissions. Photovoltaics are even displacing fossil fuels as the source of electricity generation. The European Union and China both have goals to increase the amount of photovoltaic electricity generation in their power grids. Still, to make this a reality, the industry needs more support and will need to continue growing in the years ahead. The market for photovoltaics is predicted to grow 31% from 2014 to 2017, which is greater than that of solar thermal and wind power. The Compound Annual Growth Rate (CAGR) of cumulative PV installations, including off-grid, was 34% between the year 2010 to 2020[6]

Photovoltaics is not a new technology; it's one of the oldest technologies known. It was first brought into existence by Thomas Edison and Nikola Tesla during the 1800s[7]. Solar energy has a bright future because of the technological advancement in this field and its environment-friendly nature. The most significant issue for solar energy's future is its year-round unavailability, which is compounded by its high initial cost and shortage of PV cell components. These problems can be solved by creating an efficient energy storage system and inexpensive, efficient, and plentiful PV solar cells[8].

The Sun provides 1.7×10^{22} J of energy in 1.5 days. This energy is equal to all the power that can be supplied by 3 trillion barrels of total oil resources found on Earth. As a result, the Sun's energy is much more than capable of meeting all of humanity's demands on its own. The Sun's impressive amount of energy is matched by its adaptability. The Sun's energy may be used in various ways, as shown in figure 3[9].

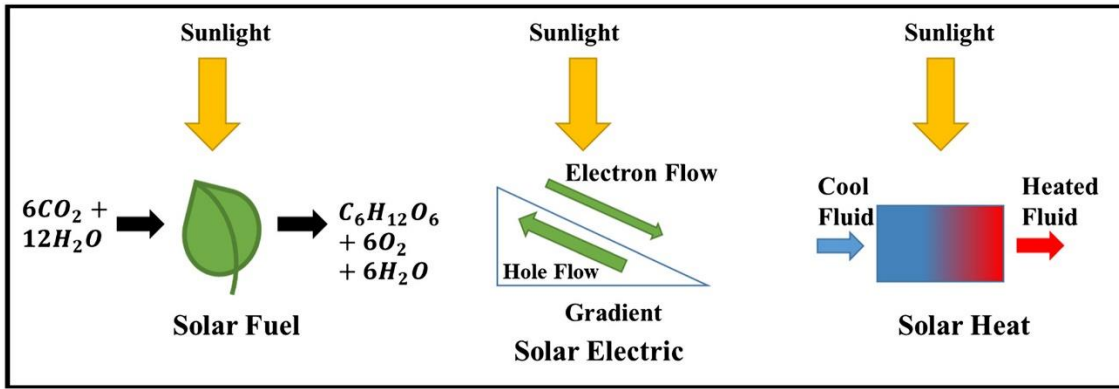


Fig.3 Three ways of converting solar energy into other forms of energy: (a) producing chemical fuel via artificial photosynthesis, (b) generating electricity by exciting electrons in a solar cell, and (c) concentrating sunlight to produce heat[8]

2.2 Multi-junction Solar Cells MJSC

Solar material plays an essential role in its efficiency. Only a limited light spectrum is absorbed depending on its bandgap. Some photons are reflected when light strikes the surface of a solar cell, whereas others pass right through. The energy of some of the absorbed photons is converted into heat. The rest have enough energy to remove electrons from their atomic bonds, resulting in charge carriers and electric current [10].

The energy required for electrons and holes to transition from the valence band to the conduction band is called a bandgap. A high-bandgap top cell is used in multi-junction devices to absorb high-energy photons while allowing lower-energy photons to pass through. After that, a material with a lower bandgap is placed beneath the high-bandgap Junction to absorb photons with lower energy (longer wavelengths), as shown in Fig. 4. Multi-junction cells typically have two or more absorbing junctions, with the theoretical maximum efficiency increasing as the number of junctions increases[11]. In multi-junction solar cells, current matching is essential. Individual component cells in multi-junction solar cells are connected in series through tunnel junctions. In general, the V_{oc} (open circuit voltage) of a multi-junction solar cell is close to the sum of the V_{ocs} of all the component cells in the multi-junction structure under the same illumination conditions.

Multiple bandgaps or junctions adjusted to absorb a specific portion of the solar spectrum are used in high-efficiency multi-junction devices to build solar cells with record efficiencies of over 45%, refer to fig. 5. The researcher invests in multi-junction (Triple Junction- refer to Fig.4) III-V solar cell research to reduce the costs of materials, manufacturing, tracking techniques, and concentration methods[12]. Multi-junction solar cells based on III-V materials (gallium arsenide (GaAs), aluminum indium phosphide (AlInP), aluminum gallium indium phosphide (AlGaInP), gallium indium phosphide (GaInP), and indium phosphide (InP), etc.) show high efficiency, exceeding 35%[11]. For satellites and space vehicles, III-V multijunction

solar cells have become the state-of-the-art photovoltaic power generator[13]

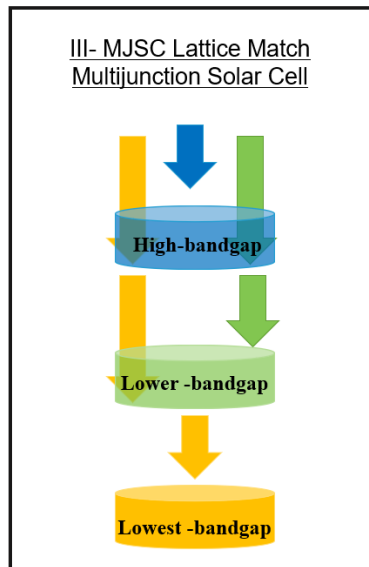


Fig.4 MJSC Lattice Match Multi-junction Solar Cell.

As a result of this method, the device only has one positive and one negative contact. Because the sub-cells of the multi-junction solar cell are connected in series, the total current is limited by the lowest current generated by one of the sub-cells[14].

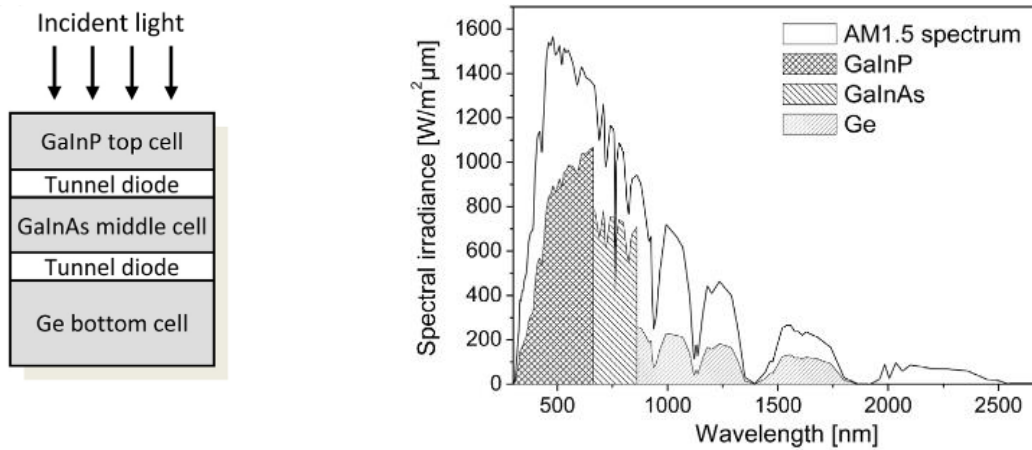


Fig.5 Schematic structure of a monolithic GaInP/GaInAs/Ge triple-junction solar cell, which represents the state-of-the-art approach for III-V multi-junction solar cells [14].

2.3 Concentrated Photovoltaic (CPV)

Typical conventional solar cells are facing many limitations on efficiency and reliability; due to certain bandgap of pn-junctions, they can only respond to particular to a specific portion of the solar spectrum and convert it into electricity, and the remaining part of the solar spectrum is just converted into heat[15].

Multi-junction solar cells, which are made up of multiple pn-junctions with different band gaps, have been used in third-generation solar cells. Each of the pn-junctions responds to a design of the solar spectrum. When multiple pn-junctions are combined, a more significant portion of the solar spectrum is absorbed and converted into electricity, while a small portion is lost as heat. However, these third-generation multi-junction solar cells are costly to manufacture due to high material costs. As a result, the concentrated photovoltaic (CPV) idea is used. Solar radiations are concentrated into a small area of solar cells using low-cost concentrators to be used cost-effectively. National Sandia Laboratories produced the first CPV system in 1976, with a capacity of 1 kW. The prototype demonstrated good performance, leading to the creation of many prototypes with capacities ranging from 0.5 to 1 kW in several nations[16]. Another pre-industrial CPV system with a capacity of 350 kW was installed in Saudi Arabia in 1981. Despite its satisfactory performance, this plant faced significant performance degradation issues due to the cell's high operating temperature. Spectrum splitting was also used to improve the CPV plant's reliability.

These efforts, however, could not help in the commercialization of CPV technology. The major cause for this was the use of silicon-based conventional single-junction solar cells, which were not designed to work in large concentrations and, as a result, were unpredictable. Even though concentrated photovoltaic (CPV) systems have the highest energy efficiency of multi-junction solar cells, the current photovoltaic market is totally based on classical single-junction PV panels. Since its beginnings, CPV technology has experienced many reliability and performance issues. Despite progress in design and reliability, CPV technology has yet to capture the attention of customers and energy planners due to its high-performance potential. In order to increase its market potential, this study discusses a compact CPV design that is high in accuracy and is intended to be installed on the rooftops of commercial and residential buildings in many areas. Furthermore, in hot weather conditions with limited beam radiation availability, the performance of a CPV system is evaluated and compared to that of different conventional PV systems.

2.3.1 Five Junction photovoltaic

With the triple-junction technology attaining a high degree of maturity and significant market demand for cells with higher output power and cost reduction at the system level, the need for a CPV solar cell with higher efficiency and a reasonable cost impact has arisen[20]. Hence Azur is working on 5J (five junctions) upright metamorphic (UMM) development, which only requires one epitaxial growth run and avoids the requirement for specific, costly processing processes (substrate removal, carrier transfer, semiconductor bonding). On the other hand, metamorphic growth risks reduced sub-cell material quality, especially for quaternary Al-containing materials such as AlInGaAs and AlInGaP, which could affect cell performance. However, AZUR, the company which manufactures these cells, proved that acceptable material quality might be achieved using UMM growth in a 4J-UMM (four junctions upright metamorphic) device for space applications that have two Al-containing sub-cells. Although UMM expansion has been identified as the most cost-effective alternative, the question of how many sub-cells will be implemented remains. Adding a fifth junction to a 4J device gives much-increased efficiency possibilities while posing only minor engineering challenges. It also has a greater Voc and lowers Jsc (short circuit current density), which is especially beneficial for CPV applications because electrical outputs are often limited by resistance losses that are quadratically proportional to current density. Considering these factors, the most promising successor to the triple junction was determined as a five-junction (5J) upright metamorphic cell design. This cell's target efficiency is 46% at high concentrations (500-1000x), with a Voc of 5.52 V and a Jsc of 9.4 A/cm² at 1000x, all under concentrating standard testing conditions (CSTC: 25°C, AM1.5d). A requirement was added to the design for optimum performance during operation circumstances, and these verified criteria at CSTC[21].

The Ge/InGaAs/AlInGaAs/AlInGaP 4J-UMM cell designed for space applications was used as a basis for the development of the 5-junction UMM cell for CPV applications. In the first step, a fifth InGaP subcell was added between the AlInGaAs and AlInGaP subcells to make a five-junction device. Due to atmospheric influences, the best bandgap combinations for CPV applications differ from those for space. A bandgap optimization for the AM1.5d spectrum was performed as a second phase. The sub-cell bandgaps of J3 and J4 should not shift into the important water absorption bands in the AM1.5d spectrum at operating temperatures up to 90°C was added as a unique criterion for this bandgap optimization. As a result, for the first batch of 5J devices, temperature coefficients for the various sub-cell materials were determined by measuring quantum efficiency at 25°C and 65°C. In order to verify the optimal bandgap combination, the same measurements were performed for the second batch of 5J devices. The tunnel diodes and sub-cells were optimized once the band gaps were fixed. This involved testing tunnel diodes for concentration factors greater than 1000 suns (both before and after heat load produced by the growth of successive solar cell layers) and designing a more

transparent tunnel diode for usage between AlInGaP and InGaP subcells. The sub-cell thicknesses will be tuned in a final iteration (to be produced) to construct a current matched 5J device with a projected efficiency of > 44% under concentration standard testing conditions (CSTC: 25°C, AM1.5d)[21].

Because CPV cells normally operate at significantly higher temperatures (up to 90°C), the J3 bandgap will shift into an absorption band, and the J4 bandgap will shift out of the absorption band under real-world conditions. As a result, current matching between the sub-cells will be highly reliant on the operation temperature, which will vary throughout the day. The second set of quantum efficiency measurements was taken at 65°C to avoid similar variations in current matching. The figure below shows the efficiency of this 5J cell as a function of concentration factor, with a maximum of 41% at 589x and efficiencies > 40.5 percent across a concentration range of 300-1150x. The relevance of current matching, which is expected for the next batch of 5J cells, is demonstrated by the slightly reduced maximum efficiency. A potential Jsc of 9.32 mA/cm² is obtained by averaging the sub-cell currents of J1 to J4, which is an increase of 8% above the current 5J device's 8.61 mA/cm². Assuming that the expected 8% rise in Jsc likewise translates into an 8% increase in efficiency, a correctly current matched cell with the current material quality might achieve an efficiency of > 44 percent [21].

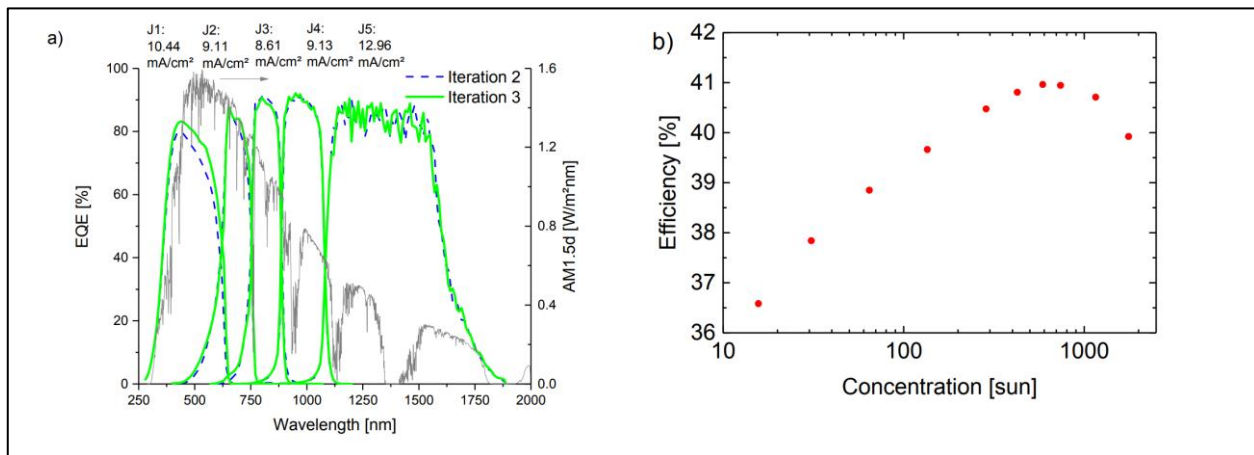


Fig.6 External Quantum Efficiency (EQE) of a third iteration 5J-UMM cell (bold, green), plotted together with the EQE of the second iteration (thin, blue) and AM1.5d reference spectrum (grey), sub-cell current densities (Jsc) indicated (a). Efficiency (η) plotted versus concentration factor (X) for the same cell (b)[21].

AZUR SPACE is now working on a 5-junction upright metamorphic (5J-UMM) cell for CPV applications. The cell design will be tuned for maximum in-system performance and a goal efficiency of 46% at 500-1000x under concentrating standard test conditions (CSTC). A bandgap optimization for the terrestrial spectrum and an optimization of the tunnel diodes and sub-cell materials were performed starting from a 4J-UMM cell created for 1 sun space applications and following the implementation of a fifth sub-cell [21]. In the future these cells will be interesting to study the reliability studies.

2.4 Space Photovoltaic

In space applications, reliability is crucial. Solar panels are critical elements exposed to the harsh environment surrounding the spaceship to supply electric power[17]. Since the beginning of the space program, scientists have known that energetic particles from the Sun and cosmic rays from other regions of space cause physical damage to silicon-based solar cells, which are the most popular and least expensive technology for satellite power generation. Because the power output of solar cells is measured virtually minute by minute during the lifetime of a satellite and other applications, thorough studies have been carried out to show how this deterioration occurs over time [18]. Protons and electrons emit radiation, which is the most common cause of solar cell breakdown; extreme temperatures, thermal cycling, atomic oxygen, debris, and other factors contribute to the deterioration[17]. Furthermore, existing qualification requirements were created for the environment surrounding the Earth. Still, the conditions for planets close to the Sun, deep-space missions, and other unknowns limit the applicability of such qualification criteria for catching the influence of extreme temperatures. The environment in space is unfriendly; PV panels suffer around eight times the degradation they would on Earth if used (except in orbits protected by the magnetosphere)[19].

2.5 Terrestrial Accelerated Life Test (ALT)

The main objective of accelerated life testing is to reduce the time taken for testing under realistic operating conditions. ALT is accomplished by putting test units under more severe stresses than those used to shorten their lifespan and save time and money during testing. Suppose the results can be extrapolated to use parameters on the assumption that the failure modes at the accelerated stress level are the same as those at the use stress level. In that case, estimations of the life under use conditions can be obtained[22].

Temperature and injected current to simulate continuous illumination are the aging factors. In this paper accelerated life test was performed at three different temperature stresses (T_1 , T_2 , and $T_3 = 119\text{ C}^\circ$, 126 C° , and 164 C°) with injecting current in darkness. The data for this test has been taken from[36].

A sample of 45 concentrated photovoltaic commercial types was tested for this research. Time was recorded for this test to reflect the lifetime of the cells. Checking the PV and I-V curves was the most direct method to identify the failure. As a result of Testing at T_2 and T_3 , which had higher temperature stresses, all the sample was fielded at a different time before ending the test. On the other hand, cells tested at T_1 lower temperature took a long time for failure to acquire; therefore, the test terminated with the failure of 9 cells only, and time was recorded for all tests after collecting all the data. A statistic equation was used to estimate the CPV lifetime based on Weibull and Lognormal data distributions using inverse power law and compare the result with Arrhenius.

2.6 Space Accelerated Life Test (ALT)

Accelerated Life Tests (ALTs) that can anticipate space solar cell reliability in a short amount of time are a must-have, the same as terrestrial solar. The Arrhenius model and the temperature ALT are commonly used to assess the reliability of III-V optoelectronic devices[23]. This work will compare the Arrhenius model result with Inverse Power low model for the space III-V solar cells. Due to the aforementioned, proper EA evaluation for each new type of III-V multi-junction solar cell utilizing precise temperature ALTs would surely improve the calculation of solar cell life expectancies. However, temperature ALT is no longer a popular operation because it requires at least three climatic rooms with adequate lighting and vacuum, as well as a specific wiring, measuring, and control system [17]. Belowares the new procedures to simulate the space condition in order to perform most accurate ALT for space solar: The data for this test has been taken from [24].

- **Oxygen-free environment.** To emulate the oxygen absence in the space environment, our climatic chamber is endowed with a gas system that injects N_2 in order to get the O_2 level below 1%.
- **Electric conditions.** The electric working conditions have been emulated by forward biasing the solar cells at the same nominal current injection level they would handle at 1xAM0. Each solar cell is biased by means of an adjustable current source 510 ± 2 mA.
- **Stress Temperatures.** They assumed a nominal temperature of $80^\circ C$, accordingly, the temperatures applied to solar cells ($150^\circ C$, $165^\circ C$, and $180^\circ C$).

2.7 Reliability and Statistic

The possibility that a product, system, or service will perform its intended function satisfactorily for a certain amount of time or in a specific environment without failure is defined as reliability. Reliability has sometimes been classified as to how CPV quality changes over time. For a multi-junction CPV, reliability is a critical issue because it is less mature than silicon PV. Building dependable products is a solution to decrease risk and ensure that the CPVs users install perform as expected for the rest of the time. The fact that survival data are generally censored or partially differentiates survival analysis from other fields of statistics. This is due to the extended period it is expected for an asset to fail. As a result, the censoring approach reduces the amount of time and money spent analyzing long-term survival data. Censoring occurs when just a portion of the information is accessible or when there is insufficient knowledge regarding the survival time of specific assets, such as CPVs.

In this research, Probability Functions Representing Reliability are the following:

- Probability density function PDF

A continuous random variable's density is a function whose value at each given sample (or point) in the sample space (the set of potential values taken by the random variable) may be understood as indicating the probability that the random variable's value will be near to that sample.

- Cumulative distribution function CDF

The likelihood that an item will fail before a particular time t is known as unreliability. Unreliability or chance of failure at a certain time: the chance that a CPV will fail at a specific time under normal operating conditions. A probability density function (PDF) is the derivative of a cumulative density function (CDF).

- Mode

The most often occurring value in a group of samples. The mode for CPV lifetime is the failure time at which most CPV fail.

- Mean

The mean, or what we commonly call the average, is the total of all the data values divided by the number of data points. The mean for CPV lifetime is the average failure time, which is usually called the meantime to failure, denoted by MTTF.

➤ Maximum likelihood estimation (MLE)

We seek to uncover general laws and principles that control the behavior under study in engineering science. These laws and principles are presented as hypotheses because they are not immediately observable. Such hypotheses regarding the structure and internal dynamics of the behavioral process of interest are mathematically represented as models, which are parametric families of probability distributions. The purpose of modeling is to determine the shape of the underlying process by evaluating the models' validity. Once a model is specified with its parameters and data have been collected, one is in a position to evaluate its goodness of fit, that is, how well it fits the observed data. Goodness of fit is assessed by finding parameter values of a model that best fits the data—a procedure called parameter estimation.

There are two general methods of parameter estimation. They are least-squares Estimation (LSE) and maximum likelihood estimation (MLE). MLE requires no or minimal distributional assumptions and is useful for obtaining a descriptive measure to summarize observed data. Still, it has no basis for testing hypotheses or constructing confidence intervals. We are using MLE because we are dealing with Censored and complete; however, others don't have the capability to handle censored samples.

The concept of maximum likelihood estimation (MLE), first introduced by R.A. Fisher in the 1920s, says that the desired probability distribution is the one that makes the observed data "most likely," implying that the parameter vector value maximizes the likelihood function must be obtained. From a statistical standpoint, the data vector $X_1, X_2, X_3, \dots, X_n$ is a random sample from an unknown population. The goal of data analysis is to identify the population that is most likely to have generated the sample. In statistics, each population is identified by a corresponding probability distribution. Associated with each probability distribution is a unique value of the model's parameter. As the parameter changes in value, different probability distributions are generated. Formally, a model is defined as the family of probability distributions indexed by the model's parameters; for example, this research focused on Weibull and lognormal distribution with their two parameters. Once data have been collected, and the likelihood function of a model given the data is determined, one is in a position to make statistical inferences about the population, that is, the probability distribution that underlies the data, given that different parameter values index different probability distributions[25]. The MLE takes form according to the parameter estimated with each statistical method used like the following.

2.7.1 Weibull Distribution

The "Weibull Distribution" in reliability engineering is one of the most commonly used distributions. It's a flexible distribution that generalizes other distributions by special choices of its parameters such as including normal and exponential distributions. Life data, model failure times, and access product reliability can be analyzed using this probability distribution. It is also applicable in a range of fields, such as economics, hydrology, biology, in addition to engineering. W. Weibull first proposed it in 1939 while studying structural strength and life data analysis, and it was formally named after him in 1951.[30].

The probability density function of a Weibull random variable has shape and scale parameters. In this research, we denote this by Weibull(α, β), where $\beta \in (0, \infty)$ is the scale parameter, and $\alpha \in (0, \infty)$ is the shape parameter, and the probability density function (PDF) is

$$f(x) = \frac{\alpha}{\beta} \left(\frac{x}{\beta}\right)^{\alpha-1} \exp\left[-\left(\frac{x}{\beta}\right)^\alpha\right], x \geq 0. \quad (1)$$

The estimating equations of the maximum likelihood estimates (MLEs) of its parameters from a complete sample of size n are

$$\frac{\sum_{i=1}^n x_i^{\hat{\alpha}_{com}} \log x_i}{\sum_{i=1}^n x_i^{\hat{\alpha}_{com}}} - \frac{1}{\hat{\alpha}_{com}} = \frac{1}{n} \sum_{i=1}^n \log x_i, \quad (2)$$

$$\hat{\beta}_{com} = \left(\frac{1}{n} \sum_{i=1}^n x_i^{\hat{\alpha}_{com}}\right)^{1/\hat{\alpha}_{com}}. \quad (3)$$

Whereas those from a censored sample of size $r < n$ are given as

$$r = (n - r)(t/\hat{\beta}_{cen})^{\hat{\alpha}_{cen}} \log(t/\hat{\beta}_{cen}) - \sum_{i=1}^r \left[1 - (x_i/\hat{\beta}_{cen})^{\hat{\alpha}_{cen}}\right] \log(x_i/\hat{\beta}_{cen})^{\hat{\alpha}_{cen}}, \quad (4)$$

$$r = (n - r)(t/\hat{\beta}_{cen})^{\hat{\alpha}_{cen}} + \sum_{i=1}^r (x_i/\hat{\beta}_{cen})^{\hat{\alpha}_{cen}}. \quad (5)$$

Moreover, the cumulative distribution function (CDF) of the Weibull distribution is given by:

$$F(x) = 1 - \exp\left[-\left(\frac{x}{\beta}\right)^\alpha\right], \geq 0 \quad (6)$$

Mean represented by:

$$\theta = \beta \Gamma\left(1 + \frac{1}{\alpha}\right) \quad (7)$$

Mode represented by:

$$\vartheta = \beta \left(\frac{\alpha-1}{\alpha}\right)^{\frac{1}{\alpha}} \quad (8)$$

2.7.2 Lognormal Distribution

A continuous probability distribution of a random variable whose logarithm is normally distributed is known as a lognormal (or lognormal) distribution in probability theory. A log-normally distributed random variable can only take positive real values. It's a useful and practical method for measurements in mathematical and engineering sciences, as well as medicine, economics, and other fields in which the lognormal is an appropriate model in life span and reliability analysis. After Francis Galton, the distribution is also referred to as the Galton distribution or Galton's distribution.

The parameter μ is called the log mean and may have any value; it is the mean of the log of life-not of life. Similarly, the parameter σ is called the log standard deviation and must be positive; it is the standard deviation of the log of life-not of life [27].

The link between the lognormal and normal distributions makes it easier to comprehend the lognormal distribution in terms of a more simple normal distribution. The (base 10) log of a variable with a lognormal distribution with parameters μ and σ has a normal distribution with mean μ and standard deviation σ . This relationship implies that a lognormal cumulative distribution function plotted against a logarithmic scale for life is identical to the distribution function for the corresponding normal distribution.

The probability density function (PDF) of the lognormal distribution is given by:

$$f(x) = \frac{1}{x\sigma\sqrt{2\pi}} \exp\left[-\frac{(\log x - \mu)^2}{2\sigma^2}\right], X \geq 0. \quad (9)$$

And cumulative distribution function (CDF) of the lognormal distribution is given by:

$$F(x) = \frac{1}{2} + \frac{1}{2} \operatorname{erf} \left[\frac{\log x - \mu}{\sqrt{2}\sigma} \right], X \geq 0. \quad (10)$$

Mean represented by:

$$\theta = \exp \left(\mu + \frac{\sigma^2}{2} \right) \quad (11)$$

Mode represented by:

$$\vartheta = \exp(\mu - \sigma^2) \quad (12)$$

MLE:

The estimating equations of the maximum likelihood estimates (MLEs) of its parameters from a complete sample of size n are

$$\hat{\mu}_{com} = \frac{1}{n} \sum_{i=1}^n \log x_i \quad (13)$$

$$\hat{\sigma}_{com} = \sqrt{\frac{1}{n} \sum_{i=1}^n (\log x_i - \hat{\mu}_{com})^2} \quad (14)$$

The estimating equations of the maximum likelihood estimates (MLEs) of its parameters from a censored sample of size n are

$$\hat{\mu}_{cen} = \frac{1}{r} \sum_{i=1}^n \log x_i + \frac{n-r}{r} \frac{\varphi(z_{cen})}{1 - \varphi(z_{cen})} \hat{\sigma}_{cen} \quad (15)$$

$$\hat{\sigma}_{cen} = \sqrt{\frac{1}{r} (\log t - \hat{\mu}_{cen}) \sum_{i=1}^r (\hat{\mu}_{cen} - \log x_i) + \frac{1}{r} \sum_{i=1}^r \frac{1}{r} (\log x_i - \hat{\mu}_{cen})^2} \quad (16)$$

Where $z_{cen} = \frac{\log t - \hat{\mu}_{cen}}{\hat{\sigma}_{cen}}$

Chapter 3

3. Result / Findings

3.1 Terrestrial PV Results

As two of the best models to fit life data, Weibull and lognormal distributions have been frequently used and compared as fitting models to several energy and electrical systems and components and materials. See for example, the performance of both in the calculations of the acceleration factors between stresses on solar cells [28], the lifetime of Organic Light-Emitting Diode, in which the entropy-based efficiency of the censored sample [30] [31] is utilized to make the comparison, the life distribution of solid-state lightning [32] [33], and the best fitting model for Lithium-Ion Batteries degraded data [34] [35]. This work adopts the Weibull distribution as the fitting model for experimental data, which was justified as clear from [36].

3.1.1 Predicting the Life at Use Conditions Using IPL and Arrhenius Models

The estimates of the Weibull parameters β and α are obtained from equations (2) and (3) when the data is complete, as in the cases of stresses T_1 and T_2 , whereas equations (4) and (5) are the correct formulas to be used when the data is censored as in the stress T_3 . The estimates of the parameters from each stressed data are reported in Table A.

Stress level	MLEs: Weibull
$T_1 = 164^\circ\text{C}/437\text{ K}$	$\beta_1 = 27.0, \alpha_1 = 2.7087$
$T_2 = 126^\circ\text{C}/399\text{ K}$	$\beta_2 = 1351.8, \alpha_2 = 2.7643$
$T_3 = 119^\circ\text{C}/392\text{ K}$	$\beta_3 = 3745.8, \alpha_3 = 2.6023$

Table A: MLEs vs. Stress Levels

The inverse power law (IPL) [37] is one of many life-stress relationships commonly used for accelerated stresses like voltage and current [36], and even when the stress is thermal, as clear from earlier works of Coffin and Manson summarized in [37]. The IPL relationship is given by:

$$l(T) = e^{aT^b} \tag{17}$$

where l : is any life measure, which is usually selected as the characteristic life for the Weibull model $l = \beta$ at which 63.2% of the units fail. a, b : are the model acceleration parameters to be calculated from data. Replacing l with β in (17), and taking log for both sides produce

$$\log\beta = a + b \log T. \tag{18}$$

The basic assumptions of IPL assume that the relationship between $\log\beta$ and $\log T$ is linear. This can be checked by just

checking that the linear correlation coefficient between the two quantities is around $r=-0.99901$ as clear from Table B.

	$T_1 = 437$	$T_2 = 399$	$T_3 = 392$
$\log T_i$	6.079933195	5.988961417	5.97126184
$\log \beta_i$	3.2958	7.2092	8.2284

Table B: The relationship between $\log \beta_i$ and $\log T_i$

In addition to that, the failure mechanism is free of stress [38], which means that the distribution shape parameter α must be fixed. This is also clear from Table A, which demonstrates that the shape parameters α_i 's under the three stresses are almost the same; hence the shape parameter α under the normal use conditions can be assumed to be around those values. Therefore, the mean value of the three scores would give a good estimate to it, which is as follows

$$\alpha = \frac{\sum_{i=1}^3 n_i \alpha_i}{\sum_{i=1}^3 n_i} = 2.7055, \quad (19)$$

The parameters a and b in (18) are the y-intercept and slope of the linear regression equation, which can be easily calculated from the usual least square method, and equation (18) will be

$$\text{IPL: } \log \beta = 274.5308 - 44.6149 \log T. \quad (20)$$

The scale parameter β is calculated by replacing T in equations (20) with the normal operating temperature of 353 K, which gives $\log \beta = 12.7991$ and, when exponentiated, provides

$$\beta = 361894.1606. \quad (21)$$

Therefore, in view of (19) and (21), the IPL-Weibull suggests that the life distribution would have the form

$$f_{\text{IPL-W}}(x) = \frac{2.7055}{361894.1606} \left(\frac{x}{361894.1606} \right)^{1.7055} \exp \left[- \left(\frac{x}{361894.1606} \right)^{2.7055} \right], x \geq 0. \quad (22)$$

In (11) $f_{\text{IPL-W}}$, denotes the Weibull PDF derived using the IPL.

On the other hand, Arrhenius life-stress relationship [39] has the form

$$\beta = e^{a+b/T}, \quad (23)$$

which when linearized gives

$$\log \beta = a + b \frac{1}{T}. \quad (24)$$

The assumptions of Arrhenius are exactly the same as those of IPL, except that the relationship between $\log \beta_i$ and $1/T_i$ must be sufficiently linear. Like the IPL case, it can be verified that the linear correlation coefficient between them is

$r=0.9993$, as can be easily checked in Table C.

	$T_1 = 437$	$T_2 = 399$	$T_3 = 392$
$1/T_i$	0.0022883	0.002506	0.0025510
$\log\beta_i$	3.2958	7.2092	8.2284

Table C: The relationship between $\log\beta_i$ and $1/T_i$

Again, the accelerating parameters a and b in equations (24) are computed using the linear regression line, and hence equation (24) will be

$$\text{Arrhenius: } \log\beta = -39.0919 + 18515.6774 \frac{1}{T} \quad (25)$$

Similarly, the scale parameter of Weibull is calculated by substituting $T = 353 \text{ K}$ in equations (25)

$$\beta = 634420.7185 \quad (26)$$

Therefore, in view of (19) and (26), the Arrhenius-Weibull suggests that the life distribution would have the form

$$f_{ARR-W}(x) = \frac{2.7055}{634420.7185} \left(\frac{x}{634420.7185}\right)^{1.7055} \exp\left[-\left(\frac{x}{634420.7185}\right)^{2.7055}\right], x \geq 0. \quad (27)$$

In (27) f_{ARR-W} denotes the Weibull PDF derived using the Arrhenius model.

To demonstrate our point, we sketch the plots of f_{IPL-W} and f_{ARR-W} . See Figure 7.

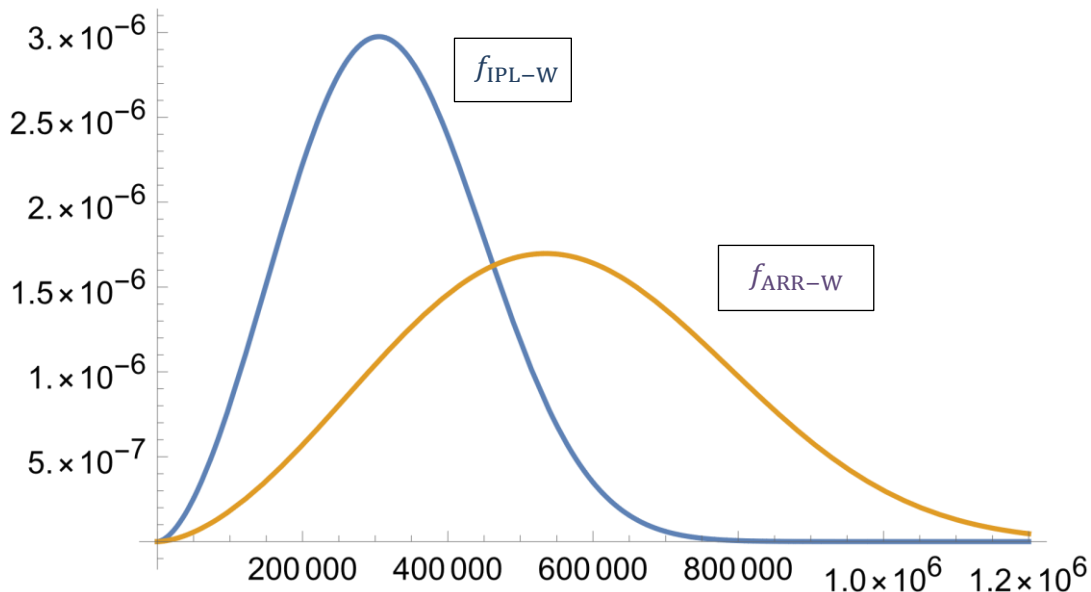


Figure 7. Sketch plots of f_{IPL-W} and f_{ARR-W}

From Figure 7. We can see that the two models are very different. For instance, it can be checked that the overlapping area between them is less than 50%, and all the descriptive measures are significantly different, as listed in Table D.

Figure	IPL	Arrhenius
Shape (α)		2.7055
Scale (β)	361894.1606	634420.7185
Mean	321849	564219
Mode	305149	534943
Standard Deviation	128319	224950

Tables D: The estimated values of some descriptive measures in hours of the solar cells' life distributions using IPL and Arrhenius models

It can be seen from Table D that if the solar cells are assumed to work 5 hours a day, the estimated mean time to failure from IPL and Arrhenius models are around 176 and 309 years, respectively. The other measures can also be checked to give completely different results between the two models.

3.2 Space PV Results

In this section, four of the most popular goodness of fit tests are applied in evaluating the appropriateness of Weibull and Lognormal distributions to the three datasets obtained from ALT. The hypothesis tests considered are Kolmogorov-Smirnov (KS), Anderson-Darling (AD), Cramer-von Mises (CvM), and Jarque-Bera (JB).

Suppose that X_1, X_2, \dots, X_n are independent identically distributed samples drawn from a continuous distribution. The task is to check whether the experimental ALT sample follows a particular distribution with CDF F_0 . This is equivalent to test the null hypothesis $H_0 : X \sim F_0(\omega)$, where ω is the parameter space of the distribution. Throughout this section, let $z_i = F_0(X_{(i)})$ for $i = 1, 2, \dots, n$ where $X_{(1)} \leq X_{(2)} \leq \dots \leq X_{(n)}$ is the corresponding ordered sample.

1. Kolmogorov-Smirnov:

Kolmogorov-Smirnov test [39] is nonparametric goodness of fit test that finds the maximum vertical distance between the empirical and theoretical distributions with test statistics (TS) defined by:

$$TS = \text{Max}(D^+, D^-),$$

$$\text{where } D^+ = \text{Max}\left(\frac{i}{n} - z_i\right), D^- = \text{Max}\left(z_i - \frac{i-1}{n}\right), i = 1, 2, \dots, n. \quad (28)$$

However, the test is not accurate when the parameters estimated from data, which is the case in this study. Thus, its modified version [40] referred to as the Lilliefors test is used instead.

2. Anderson-Darling:

Anderson and Darling [41] [42] developed a goodness of fit test for completely specified distributions with known parameters provided by:

$$TS = -n - \frac{\sum_{i=1}^n (2i-1)(\text{Log}(z_i) + \text{Log}(1-z_{n+1-i}))}{n}. \quad (29)$$

The test is used to test a family of distributions, including Weibull and lognormal distribution, where the distribution parameters should be estimated and considering the amendment of the test statistic or its critical values.

3. Cramer-von Mises:

The Cramer-von Mises test is one of the most effective goodness of fit tests [43]. The original test established by [44], given as:

$$TS = \frac{1}{12n} + \sum_{i=1}^n \left(\frac{2i-1}{2n} - z_i\right)^2. \quad (30)$$

4. Jarque-Bera:

Jarque-Bera is deemed as a strong evidence for lognormality [45] [46] [47] when the logarithm of the sample is proved to be normally distributed. Its test statistic is governed by:

$$TS = n\left(\frac{s^2}{6} + \frac{(k-3)^2}{24}\right), \quad (31)$$

where s and k are skewness and kurtosis of the log-transformed data. The Jarque-Bera is usually used as an auxiliary test after taking the approval of the above three tests. This test is not applicable to Weibull distribution.

The results of the tests are shown in Tables E-G for the three data sets T_1 , T_2 and T_3 , respectively. The distribution that scores a higher p-value is favorable as it reflects a closer fit to the data. A significance level of 0.05 is assumed. The following abbreviations are used in the tables, TS: Test statistic, CV: Critical Value, PV: p-value, W: Weibull, and L: Lognormal.

Tests	Weibull			Lognormal			Better Fit
	TS	CV	PV	TS	CV	PV	
KS	0.28	0.38	0.45	0.28	0.39	0.48	L
AD	0.46	0.66	0.24	0.43	0.65	0.29	L
CvM	0.08	0.11	0.23	0.07	0.11	0.23	Both
JB		NA		0.57	0.86	0.29	

Tables E: Goodness of fit tests summary for the data set T_1

Tests	Weibull			Lognormal			Better Fit
	TS	CV	PV	TS	CV	PV	
KS	0.28	0.35	0.28	0.28	0.36	0.28	Both
AD	0.44	0.69	0.28	0.51	0.68	0.18	W
CvM	0.07	0.11	0.30	0.09	0.12	0.25	W
JB		NA		0.69	1.23	0.24	

Tables F: Goodness of fit tests summary for the data set T_2

Tests	Weibull			Lognormal			Better Fit
	TS	CV	PV	TS	CV	PV	
KS	0.37	0.35	0.03	0.34	0.36	0.09	L
AD	0.70	0.69	0.04	0.60	0.69	0.09	L
CvM	0.13	0.03	0.03	0.10	0.12	0.24	L
JB		NA		1.24	1.22	0.04	

Tables G: Goodness of fit tests summary for the data set T_3

From Tables E-G, one can see that both distributions fit ALT data sets well. From Table E, it can be seen that KS and CvM tests recommend Weibull, whereas AD and JB recommend lognormal. However, both Tables G and F strongly recommend lognormal as the preferred model. In summary, it is clear that the lognormal distribution is the best among both.

3.2.1 Predicting the Life at Use Conditions Using Arrhenius Model and IPL

From the previous section, we see that the lognormal is a better fit to the experimental data. Therefore, in this section, we use it instead of Weibull to predict the life at use conditions. Here we apply both Arrhenius and inverse power law life-stress relationships to perform this task.

Stress level	MLEs
$T_1 = 180\text{ }^\circ\text{C}/453\text{ K}$	$\mu_1 = 9.63, \sigma_1 = 0.614$
$T_2 = 165\text{ }^\circ\text{C}/438\text{ K}$	$\mu_2 = 10.25, \sigma_2 = 0.921$
$T_3 = 150\text{ }^\circ\text{C}/423\text{ K}$	$\mu_3 = 11.36, \sigma_3 = 0.536$

Table H: MLEs vs. Stress Levels

A. Arrhenius:

As a general trend, the empirical model vastly used to describe thermal acceleration in the life-stress relationship is the Arrhenius model [48]. The Arrhenius physical model is governed by

$$l(I) = e^{a+b/T} , \quad (32)$$

where:

l : is any life measure, I : represents the stress, which is the temperature, and a, b : are the model acceleration parameters to be determined.

The linear form of the Arrhenius model is derived by taking log to equation (32) and given by

$$\log l = a + b \frac{1}{T} \quad (33)$$

The common life measure for Weibull is assumed to be ($l = \beta$) , which is the 63rd percentile of the distribution, whereas, it is the median ($l = e^\mu$) for Lognormal distribution [38]. Hence, the Arrhenius–Lognormal models can respectively be written as

$$\mu = a + b \frac{1}{T} \quad (34)$$

The key assumptions that validate using Arrhenius stress relationship models (34) are that (A1) The three datasets must acceptably fit the lifetime model Weibull or lognormal, which has been confirmed in Section IV.

(A2) The failure mechanism is free of the stresses T_1, T_2, T_3 and the use stress, where the applied stress only changes the scale of the lifetime. This means that the life distributions of the three stresses and the use stress must have the same shape parameters

$$\sigma = \sigma_1 = \sigma_2 = \sigma_3 \quad (35)$$

This is a strong assumption that in practical applications is impossible to precisely hold, and hence, the weighted average of the shape parameters at all stresses would be a reasonable estimate to that at use conditions

$$\sigma = \frac{\sum_{i=1}^3 n_i \sigma_i}{\sum_{i=1}^3 n_i} = 0.6958, \quad (36)$$

where $n_1 = 4, n_2 = n_3 = 5$ as clarified in Section II.

(A3) The relationship between μ_i and $1/T_i$ must be sufficiently linear. This can be verified using the linear correlation coefficient (r) between μ_i and $1/T_i$, which is in this case, $r=0.99$, as can be easily checked from Table I.

	T_1	T_2	T_3
$1/T_i$	0.0022075	0.0022831	0.0023641
μ_i	9.63	10.25	11.36

Table I: The relationship between $\frac{1}{T_i}$ and μ_i

The accelerating parameters a and b in equation (34) are obtained using the least square method as $a = -14.9065$, $b = 11081.4$, and thus the (34) takes the following forms.

$$\mu = -14.9065 + 11081.4 \frac{1}{T} \quad (37)$$

Accordingly, the activation energy would be $E = 8.6173303 \times 10^{-5} \times b = 0.96 \text{ eV}$. The scale parameter μ under possible use conditions (80 C, 100 C, 120 C and 130 C) are then calculated by respectively substituting $T = 353 \text{ K}, 373 \text{ K}, 393 \text{ K}$ and 403 K in equation (37), and thus, the respective meantime to failure, can be calculated by substituting the resulting μ 's in the mean formula $e^{\mu + \sigma^2/2}$ of the lognormal distribution under shape parameter $\sigma = 0.6958$. The results are reported in Table J.

Use Stress Levels	The scale parameter μ	Mean time to failure
80 °C/353 K	16.485568	18395871 h (2100 y)
100 °C/373 K	14.8023472	3417487 h (390 y)
120 °C/393 K	13.2904466	753523 h (86 y)
130 °C/403 K	12.5907705	374310 h (43 y)

Table J: The estimates of the scale parameter using IPL-lognormal model for several use conditions

B. Inverse power law:

The inverse power law (IPL) [49] is given by:

$$l(I) = e^{aT^b} \quad (38)$$

The inverse power law can be expressed as a straight line after taking log to (38)

$$\log l = a + b \log T. \quad (39)$$

Hence, the IPL–Lognormal models can be written as

$$\mu = a + b \log T. \quad (40)$$

Similar to the The basic assumptions [31] that validate using any of the life-stress relationship model (40) are:

(A1) The data for the three stress levels must acceptably fit the lognormal, which is proved in the previous section.

(A2) The failure mechanism of is free of stress and only rescaled with the change in the stresses T_1 , T_2 and T_3 . This means that the life distributions of the three stresses (and the use stress) must have the same shape parameters which is calculated in (40).

(A3) The relationships between μ_i and $\log T_i$ must be sufficiently linear. This can be verified by calculating the linear correlation coefficient (r). In this case, $r=-0.99$, see Table K.

	T_1	T_2	T_3
$\log (T_i)$	2.6561	2.6415	2.6263
μ_i	9.63	10.25	11.36

Table K: The relationship between $\log (T_i)$ and μ_i

The acceleration parameters a and b in (40) are obtained using the usual least square method, and hence (40) can be written as follows.

$$\mu = 164.201 - 25.2865 \log T. \quad (41)$$

The scale parameter μ under possible use conditions (80 C, 100 C, 120 C and 130 C) are then calculated by respectively substituting $T = 353 K, 373 K, 393 K$ and $403 K$ in equation (41), and thus, the respective meantime to failure, can be calculated by substituting the resulting μ 's in the mean formula $e^{\mu+\sigma^2/2}$ of the lognormal distribution under shape parameter $\sigma = 0.6958$. The results are reported in Table L.

Use Stress Levels	The scale parameter μ	Mean time to failure
80 °C/353 K	15.858555	9826804 h (1122 y)
100 °C/373 K	14.465007	2438945 h (278 y)
120 °C/393 K	13.144263	651044 h (74 y)
130 °C/403 K	12.508891	344883 h (39 y)

Table L: The estimates of the scale parameter using the Arrhenius-lognormal model for several use condition

Chapter 4

4. Discussion

This part discusses the results of the CPV lifetime model based on inverse power law using Lognormal and Weibull distributions based on the sample derived from the ALT tests.

Temperature and injected current that simulates continuous illumination are the aging factors. In this work for terrestrial solar cells accelerated life test was performed at three different temperature stresses (T1, T2, and T3 = 119 C°, 126 C°, and 164 C°) with injecting current in darkness. The data for this work has been adapted from as mentioned in previous sections. A sample of 45 concentrated photovoltaic commercial types was tested for this research. Time was recorded for this test to reflect the life-time of the cells. Checking the PV, and I-V curves was the most direct method to identify the failure. As a result of testing at T2 and T3, which had higher temperature stresses, all the samples failed but at different times and before ending the test. On the other hand, cells tested at T1 lower temperature took a long time for failure to acquire; therefore, the test terminated with the failure of 9 cells only, and time was recorded for all tests after collecting all the data.

On the other hand, 20 sample of space solar was equally segregated and exposed to three temperature levels; T1: 180°C (453 K), T2: 165°C (438 K), and T3: 150°C (423 K). Dark I–V curves were used to characterize the evolution of the solar cell's performance by analyzing the voltage variation at a current injection level similar to their photocurrent under 1xAM0, which corresponds to 510 mA for these solar cells in particular. Before concluding the test, samples failed at different times. In both cases, the CPV lifetime is estimated based on Weibull and Lognormal distributions using inverse power law and compare the result with the so-called Arrhenius model.

From the above results for terrestrial and space solar results based on Inverse power law and comparing it the Arrhenius model we can conduct that, first Inverse Power Law can be used to predict and estimate the CPV lifetime but there is no clear conclusion of which way is the best. Secondly, the lifetime of space CPV and Terrestrial are following approximately the same models.

Chapter 5

5.1 Conclusion

The efficiency of CPV has attracted a lot of attention. However, the issue of CPV reliability and robustness remains unresolved. Under the umbrella of reliability, lifetime models play a critical role in gaining insights into CPV lifespan features.

In conclusion, for this work, depending on the CPV failure mechanism comparing between Arrhenius and inverse power law, both models can provide an excellent result to predict the lifetime of CPV. ALT tests for commercial concentrator lattice match triple-junction GaInP/GaInAs/Ge cells were performed on the data used as the CPVs sample. Our study believes that the CPV lifetime could be in between the two results of Arrhenius and inverse power law.

As a result, we found that the lifetime estimates of CPV obtained from Inverse Power Law and Arrhenius model are significantly different, therefore, an appropriate estimate for the lifetime of CPV might be taken as a value in the middle of the two estimates. More analysis and evidence are needed to understand the failure mechanism of CPV, and discussion needs to be added to this work to conclude the correct method of predicting the lifetime as it is a new technology. Current qualification criteria have been designed for the environment surrounding the Earth. Still, the conditions for planets close to the Sun, deep-space missions, and other unknowns limit the applicability of such qualification requirements for capturing the effects of extreme temperatures.

References

- [1] S. Philipps and W. Warmuth, Photovoltaics Report. Freiburg, Baden-Württemberg: Fraunhofer Institute for Solar Energy Systems, ISE, 2020.
- [2] C. Algora et al., "Reliability," in Handbook of Concentrator Photovoltaic Technology, John Wiley & Sons, Ltd, 2016.
- [3] "Performance evaluation of single multi-junction solar cell for high concentrator photovoltaics using minichannel heat sink with nanofluids | Elsevier Enhanced Reader."
- [4] "National Renewable Energy Laboratory (NREL)." <https://www.nrel.gov/index.html> (accessed May 09, 2021).
- [5] V. Orlando et al., "Temperature Accelerated Life Test and Failure Analysis on Upright Metamorphic Ga_{0.37}In_{0.63}P/Ga_{0.83}In_{0.17}As/Ge Triple Junction Solar Cells," Prog. Photovolt. Res. Appl., vol. 28, no. 2, pp. 148–166, 2020.
- [6] C. Algora et al., "Reliability," in Handbook of Concentrator Photovoltaic Technology, John Wiley & Sons, Ltd, 2016. – REPETED
- [7] I. T. W. D. N. D. July 10, 2017UPDATED: July 10, and 2017 17:12 Ist, "Nikola Tesla and Thomas Edison: The war of currents and the search for truth," India Today. <https://www.indiatoday.in/education-today/gk-current-affairs/story/tesla-edison-history-1023468-2017-07-10> (accessed Nov. 11, 2021).
- [8] M. D. K. L. N, "Solar energy—A look into power generation, challenges, and a solar-powered future", (05 November 2018).
- [9] Harald Cramér (1928) On the composition of elementary errors, Scandinavian Actuarial Journal, 1928:1, 13–74, DOI: 10.1080/03461238.1928.10416862
- [10] "Solar Performance and Efficiency," Energy.gov. <https://www.energy.gov/eere/solar/solar-performance-and-efficiency> (accessed Nov. 11, 2021).
- [11] "Multijunction III-V Photovoltaics Research," Energy.gov. (accessed Nov. 11, 2021).
- [12] "Multijunction III-V Photovoltaics Research," Energy.gov. <https://www.energy.gov/eere/solar/multijunction-iii-v-photovoltaics-research> (accessed Nov. 11, 2021).
- [13]] R. M. Daniel C. Law, Kenneth M. Edmondson, Hojun Yoon, Geoffrey S. Kinsey, Dimitri D. Krut, James H. Ermer, Peter Hebert, B. Terence Cavicchi, and Nasser H. Karam "DVANCED III-V MULTIJUNCTION CELLS FOR SPACE" (June 2006).
- [14] J. Appl. Phys. 129, 240901 (2021); "Multi-junction solar cells paving the way for super high-efficiency", (23 June 2021).
- [15] M. Burhan, M. W. Shahzad, and K. C. Ng, "Concentrated Photovoltaic (CPV): From Deserts to Rooftops," in Advances in Sustainable Energy, A. Vasel and D. S.-K. Ting, Eds. Cham: Springer International Publishing, 2019, pp. 93–111.
- [16] "Concentrator photovoltaics," Wikipedia. Oct. 24, 2021. Accessed: Nov. 27, 2021.

- [17] W. Guter et al., "Space Solar Cells – 3G30 and Next Generation Radiation Hard Products," E3S Web of Conferences, vol. 16, p. 03005, Jan. 2017.
- [18] R. H. van Leest, D. Fuhrmann, A. Frey, M. Meusel, G. Siefer, and S. K. Reichmuth, "Recent progress of multi-junction solar cell development for CPV applications at AZUR SPACE," Fes, Morocco, 2019, p. 020007.
- [19] R. Hoheisel, F. Dimroth, A. W. Bett, Scott R. Messenger, P. Jenkins, R. J. Walters "Electroluminescence analysis of irradiated GaInP/GaInAs/Ge space solar cells". (January 2013).
- [20] M. Sengupta, A. Habte, C. Gueymard, S. Wilbert, and D. Renné, "Best Practices Handbook for the Collection and Use of Solar Resource Data for Solar Energy Applications: Second Edition", (January 2017).
- [21] "Space-based solar power," Wikipedia. Mar. 15, 2022. Accessed: Apr. 04, 2022.
- [22] N. Nuñez, M. Vazquez, V. Orlando, P. Espinet- González, and C. Algora, "Semi- quantitative temperature accelerated life test (ALT) for the reliability qualification of concentrator solar cells and cell on carriers," Prog. Photovolt. Res. Appl., vol. 23, no. 12, pp. 1857–1866, 2015.
- [23] P. Vassiliou, A. Mettas, and P. Vassiliou, "RF #2003RM-100: page i RF 2003 Annual RELIABILITY and MAINTAINABILITY Symposium Understanding Accelerated Life-Testing Analysis."
- [24] N. Nuñez et al., "Estimation of activation energy and reliability figures of space lattice-matched GaInP/Ga(In)As/Ge triple junction solar cells from Temperature Accelerated Life Tests," Solar Energy Materials and Solar Cells, vol. 230, p. 111211, Sep. 2021.
- [25] I. J. Myung, "Tutorial on maximum likelihood estimation," Journal of Mathematical Psychology, vol. 47, no. 1, pp. 90–100, Feb. 2003.
- [26] "History Of Weibull Distribution" (UKEssays.com, April 2022).
- [27] Nelson, W. B. (2003). Applied life data analysis (Vol. 521). John Wiley & Sons.
- [28] Kittaneh, O. A., Ammach, S., Helal, S., Barkat, E., & Majid, M. A. (2022). A Comparative Study Between Lognormal and Weibull Distributions in Modeling Commercial Concentrator III–V Triple-Junction Solar Cells Lifetimes. International Journal of Renewable Energy Research (IJRER), 12(1), 547-556.
- [29] O. Kittaneh, S. Helal, H. Almorad, H. Bayoud, G. Abufoudeh, and M. Majid, "Preferable Parametric Model for the Lifetime of the Organic Light-Emitting Diode Under Accelerated Current Stress Tests," IEEE Transactions on Electron Devices, vol. PP, pp. 1–7, Jul. 2021.
- [30] Kittaneh, O. A., Almorad, H., Helal, S., & Majid, M. A. (2021). On the efficiency of type I censored samples. IMA Journal of Mathematical Control and Information, 38(2), 743-753.
- [31] Kittaneh, O. A., Shehata, M., & Majid, M. A. (2018, February). An efficient censoring scheme for lifetime of connected solid-state lighting based on entropy measures. In 2018 15th Learning and Technology Conference (L&T) (pp. 35-39). IEEE.
- [32] O. A. Kittaneh, M. Shehata, and M. A. Majid, "An efficient censoring scheme for lifetime of connected solid-state lighting based on entropy measures," in 2018 15th Learning and Technology Conference (L&T), Jeddah, Feb. 2018, pp. 35–39.
- [33] O. A. Kittaneh and M. A. Majid, "Comparison of two-lifetime models of solid-state lighting based on sup-entropy," Heliyon, vol. 5, no. 10, p. e02551, Oct. 2019.

- [34] T. Mouais, O. Kittaneh, and M. Majid, "Choosing the Best Lifetime Model for Commercial Lithium-Ion Batteries," *The Journal of Energy Storage*, vol. 41, p. 102827, Sep. 2021.
- [35] T. Mouais, O. Kittaneh, and M. Abdulmajid, "The Effects of Electrode Physical Parameters on the Statistical Life Models of Li-Ion Battery," Apr. 2021, pp. 1–5.
- [36] P. Espinet-González et al., "Temperature accelerated life test on commercial concentrator III-V triple-junction solar cells and reliability analysis as a function of the operating temperature: Temperature accelerated life test," *Prog. Photovolt: Res. Appl.*, vol. 23, no. 5, pp. 559–569, May 2015.
- [37] P. Espinet-González et al., "Preliminary temperature accelerated life test (ALT) on III-V commercial concentrator triple-junction solar cells," Jun. 2012.
- [38] Nelson, Wayne, *Accelerated Testing: Statistical Models Test Plans and Data Analyses* John Wiley & Sons, Inc., New York, 1990.
- [39] F. J. Massey, "The Kolmogorov-Smirnov Test for Goodness of Fit," p. 12, 2020.
- [40] H. W. Lilliefors, "On the Kolmogorov-Smirnov Test for Normality with Mean and Variance Unknown," *Journal of the American Statistical Association*, vol. 62, no. 318, pp. 399–402, Jun. 1967.
- [41] T. W. Anderson and D. A. Darling, "Asymptotic Theory of Certain 'Goodness of Fit' Criteria Based on Stochastic Processes," *The Annals of Mathematical Statistics*, vol. 23, no. 2, pp. 193–212, Jun. 1952.
- [42] T. Zubayraev, "Asymptotic Analysis for U-Statistics and Its Application to Von Mises Statistics," *OJS*, vol. 01, no. 03, pp. 139–144, 2011.
- [43] J. Bortz, G. A. Lienert, and K. Boehnke, *Verteilungsfreie Methoden in der Biostatistik*. Springer-Verlag, 2013.
- [44] H. Cramér, "On the composition of elementary errors," *Scandinavian Actuarial Journal*, vol. 1928, no. 1, pp. 13–74, Jan. 1928.
- [45] C. M. Jarque and A. K. Bera, "Efficient tests for normality, homoscedasticity and serial independence of regression residuals," *Economics Letters*, vol. 6, no. 3, pp. 255–259, 1980.
- [46] Jarque, C. M., & Bera, A. K. (1980). Efficient tests for normality, homoscedasticity and serial independence of regression residuals. *Economics letters*, 6(3), 255-259.
- [47] A. K. Bera and C. M. Jarque, "Efficient tests for normality, homoscedasticity and serial independence of regression residuals. Monte Carlo Evidence," *Economics Letters*, vol. 7, no. 4, pp. 313–318, 1981.
- [48] Escobar, L. A., & Meeker, W. Q. (2006). A review of accelerated test models. *Statistical science*, 552-577.
- [49] Jarque, C. M., & Bera, A. K. (1980). Efficient tests for normality, homoscedasticity and serial independence of regression residuals. *Economics letters*, 6(3), 255-259.

List of Tables

Table A. MLEs vs. Stress Levels

Table B. The relationship between $\log\beta_i$ and $\log T_i$

Table C. The relationship between $\log\beta_i$ and $1/T_i$

Table D. The estimated values of some descriptive measures in hours of the solar cells' life distributions using IPL and Arrhenius models

Tables E: Goodness of fit tests summary for the data set T_1

Tables F: Goodness of fit tests summary for the data set T_2

Tables G: Goodness of fit tests summary for the data set T_3

Table H: MLEs vs. Stress Levels

Table I: The relationship between $\frac{1}{T_i}$ and μ_i

Table J: The estimates of the scale parameter using IPL-lognormal model for several use conditions

Table K: The relationship between $\log(T_i)$ and μ_i

Table L: The estimates of the scale parameter using Arrhenius-lognormal model for several use conditions

List of figures

Figure 1. Concentrated Photovoltaics general diagram

Figure 2. NREL highest confirmed conversion efficiencies for research cells for a range of photovoltaic technologies plotted from 1976 to the present

Figure 3. Three ways of converting solar energy into other forms of energy

Figure 4. MJSC Lattice Match Multi-junction Solar Cell.

Figure 5. Schematic structure of a monolithic GaInP/GaInAs/Ge triple-junction solar cell, which represents the state-of-the-art approach for III-V multi-junction solar cells

Figure 6. External Quantum Efficiency (EQE) of a third iteration 5J-UMM cell

Figure 7. Sketch plots of f_{IPL-W} and f_{ARR-W}

List of Terms

<i>Thesis Terms List</i>	
PV	Photovoltaic
CPV	Concentrated Photovoltaic
CSP	Concentrating Solar thermal – power basis
MJ	Multi-junction
NREL	National Renewable Energy Laboratory
ALT	Accelerated Life Test
MJSC	Multi-Junction Solar Cells
III-V	Triple Junction
MBE	Molecular-Beam Epitaxy
MOCVD	Metal-Organic Chemical-Vapor Deposition
PDF	Probability Density Function
MLE	Maximum Likelihood Estimates
CDF	Cumulative Distribution Function

Appendices

The 14th Annual IEEE GreenTech Conference March 30th - April 3rd 2022 Houston, TX /
ieeegreentech.org

Life Distribution of Commercial Concentrator III-V Triple-Junction Solar Cells in View of Inverse Power Law and Arrhenius Life-stress Relationships: Dunya Dennah (Effat, Saudi Arabia); Salwa Bilal Ammach (Effat University, Saudi Arabia); Mohammed Abdul Majid (Effat University, An Nazlah Al Yamaniyyah, Saudi Arabia); Enfel Barkat (University of Colorado Denver, USA)

2022 IEEE Green Technology Conference Program Schedule	
Wednesday, March 30	
■ INTRODUCTION & OPENING REMARKS: 11:15-11:30 ■	
LUNCH: 11:30-13:00	
KEYNOTE SPEAKER: A GLOBAL PERSPECTIVE ON SUSTAINABLE ENERGY AND TRANSPORTATION MEHRDAD (MARK) EHSANI, PHD, TEXAS A&M UNIVERSITY: 11:30-12:30	
Session 1 - Power Electronics and its Control: 13:00-14:30 [Session Chair: Kenneth Rice]	
Harmonic Analysis of Single-Phase Rooftop Solar PV Systems with Non-Linear Loads: Syed Muhammad Ahsan & Hassan Abbas Khan (Lahore University of Management Sciences, Pakistan) System Size and Loss of Power Supply Probability Reduction Through Peer-to-Peer Power Sharing in DC Microgrids: Reesha Arshad (Lahore University of Management Sciences, Pakistan); Muhammad Anees (North Carolina State University, USA); Mashood Nasir (CLERENS, Belgium); Hassan Abbas Khan (Lahore University of Management Sciences, Pakistan) Power Smoothing of Battery Integrated Solar PV Output Using Meta-Heuristic Optimization: Ammar Atif, Khalid Abdullah Khan and Muhammad Khalid (King Fahd University of Petroleum and Minerals, Saudi Arabia) Using an AFD's Inverter to Improve Line-connected Induction Motor Power Factor within Integrated Control Gear: Stan R Simms (Eaton & Eaton Electrical, USA); Gabriel T Braga (PWP Lab, Brazil); Steven Johnston (Eaton, USA); Thomas A Farr (Eaton Corporation, USA) PV to Vehicle, PV to Grid, Vehicle to Grid, and Grid to Vehicle Micro Grid System Using Level Three Charging Station: Afshin Balal & Michael Giesselmann (Texas Tech University, USA)	
BREAK: 14:30-15:00	
Session 2 - Virtual Session: 15:00 - 16:00 [Session Chair: Bradley Updyke]	
Sequence Hopping Algorithm for Securing IEC 61850 GOOSE Messages: Tarek Youssef (University of West Florida, USA); Mohamad El Hariri (Colorado School of Mines, USA); Osama Mohammed (Florida International University, USA); Celina Wilkerson (Colorado School of Mines, USA) Life Distribution of Commercial Concentrator III-V Triple-Junction Solar Cells in View of Inverse Power Law and Arrhenius Life-stress Relationships: Dunya Dennah (Effat, Saudi Arabia); Salwa Bilal Ammach (Effat University, Saudi Arabia); Mohammed Abdul Majid (Effat University, An Nazlah Al Yamaniyyah, Saudi Arabia); Enfel Barkat (University of Colorado Denver, USA) Effect of Glucose Concentration and Oxygen Regulation on Biohydrogen Yield Using Microalgae and Activated Sludge Co-culture - A Source of Green Energy and Waste Energy Utilization: Muhammad Asad Javed & Ashraf Aly Hassan (United Arab Emirates University, United Arab Emirates) A Fairness-Based Distributed Energy Coordination for Voltage Regulation in Distribution Systems: Shiva Poudel , Monish Mukherjee & Andrew P. Reiman (Pacific Northwest National Laboratory, USA)	
Session 3 - Cybersecurity: 16:00 - 17:00 [Session Chair: Sameh Eisa]	
Load Margin Constrained Moving Target Defense Against False Data Injection Attacks: Hang Zhang , Noah Fulk, Bo Liu, Lawryn Edmonds, Xuebo Liu & Hongyu Wu (Kansas State University, USA) Detection of Cyber Attacks in Grid-tied PV Systems Using Dynamic Watermarking: Hasan Ibrahim & Jaewon Kim (Texas A&M University, USA); Prasad Enjeti (Texas A&M, USA); P R Kumar and Le Xie (Texas A&M University, USA)	
■ CONFERENCE WELCOME DINNER 18:00 ■	
Thursday, March 31	
BREAKFAST: 08:00-08:30	
Session 4 - Renewable Energy Resources: 08:30 - 10:00 [Session Chair: Afsin Balal]	
Novel Non-Tracking Fiber Optic Solar Concentrator: Luis R Rosario , Jordyn K Sibert, Luisana E Padron, Daniel Guerra & Jeffrey D Gleasman (USA) Techno-Economic Study of Marine Hydrokinetic Turbines for Electricity Production over the US Gulf Stream: Nicolas Rene Sockeel & Amber Galeana (University North Carolina Charlotte, USA); Robert Cox (The University of North Carolina at Charlotte, USA) PV Fuzzy Model Based on V-I Curves to be Implemented in an Intelligent Sensor: José Rivera-Mejía , Vicente Medina-Rodríguez & Rocío Eduwiges Quiñonez-Moreno (Instituto Tecnológico de Chihuahua del TECNM, Mexico) Performance Study of an Optimized Lead-free Cs3Sb2I9-based Perovskite Solar Cell Using SCAPS-1D: Shamik Datta (University of Texas, Rio Grande Valley, USA); Md Maruf Hossain & Samiha Nuzhat (Shahjalal University of Science and Technology, Bangladesh); Ananya Debnath (Chittagong University of Engineering and Technology, Bangladesh); Hasina Huq (The University of Texas Rio Grande Valley, USA) Comprehensive Characterization of the Periodic Attractors Problem in the Wind Turbine Control System: Sameh Eisa (University of Cincinnati, USA)	
BREAK: 10:00-10:15	
Session 5 - Power System & Protocol Management: 10:15 - 11:30 [Session Chair: Xingpeng LI]	
Cluster Automation System for Dynamic Grid Control at Distribution Level: Daniel Holtschulte, Andreas Schmelter, Tawichai Premgamone , Egon Ortjohann, Jan Kortenbruck & Shashank Varada (South Westphalia University of Applied Sciences, Germany)	